Nanostructures

DOI: 10.1002/anie.200804798

Cobalt Growth on the Tips of CdSe Nanorods**

Jérôme Maynadié, Asaf Salant, Andrea Falqui, Marc Respaud, Ehud Shaviv, Uri Banin, Katerina Soulantica, and Bruno Chaudret*

The successful implementation of nanocrystals in real applications greatly depends on the possibility to integrate them into macroscopic systems, which is a technological challenge. Progress in the control of size, shape, organization, and composition, which has been achieved by wet chemical methods,[1] allows increasingly precise control of nanocrystal characteristics. Indeed, an emerging direction in nanomaterials research is the transition from simple to multifunctional nanocrystals, which serve several parallel purposes simultaneously by combining two or more constituents.[2]

One type of multifunctional nanocrystals consists of nanoobjects combining at least two discrete, nonconcentric, chemically different domains. Several materials have been successfully combined recently to give such hybrid nanoparticles.[3] The most widely employed method is the use of nanocrystals of one material as templates for heterogeneous growth of a second material.[4] Anisotropic nanocrystals, which display interesting shape-dependent properties, offer the additional possibility to selectively position the second constituent at a specific location.[3a,b,5] The use of nanorods or tetrapods as growth templates has permitted the synthesis of anisotropic hybrid nanoparticles. This progress may in turn offer additional opportunities for applications in which topological recognition of the nanoparticle is important.[6] The combination of a magnetic and a semiconducting domain on the same nano-object offers the opportunity to use the magnetic properties to direct the positioning of the semiconductors to a predefined location or to organize them over large areas by application of an external magnetic field. Provided that the magnetic and optical properties of each functionality are conserved in the final nanoobject, several applications can be envisaged, for example, for biological labelling[3e,f] or in electrooptic devices.[7]

The majority of magnetic–semiconducting hybrid nanoparticles reported to date include magnetic oxides. Additionally, hybrid structures such as CdS–FePt in which both the luminescent and the magnetic properties of the isolated constituents are still manifested in the final object were reported.[3d] During the course of this study, the synthesis of magnetic PtNi and PtCo nanospheres on the tips of CdS nanorods was reported, but without description of their magnetic or optical properties.[8]

Work by Mokari et al. has focused on the synthesis of gold-tipped CdSe nanorods,[3a,b] while Wetz et al. have synthesized gold-tipped and gold-decorated Co nanorods.[5b] In these cases, the specific reactivity of the rod apex regions allowed for selective growth of the metal tips. Herein, we report the synthesis of CdSe–Co nanorod–nanosphere hybrid nanocrystals (NCs1) through the growth of cobalt nanospheres on preformed CdSe nanorods, further exploiting the advantageous feature of selective reactivity at the apex regions. Moreover, we describe the anisotropic growth of the initially formed Co nanospheres, which leads to CdSe–Co nanorod–nanorod hybrid nanocrystals (NCs2). Anisotropic growth of heterostructures in solution is very rare.[9] To our knowledge these are the first magnetic-metal/semiconductor nanorod–nanorod heterostructures prepared by colloidal methods. Preliminary studies on the magnetic and optical properties of the hybrid nanoparticles are also described.

The selective growth of cobalt nanostructures on the tips of CdSe nanorods is achieved by addition of $[Co(\eta^4\text{-}C_8H_{12})(\eta^3\text{-}C_8H_{13})]$ to a toluene solution containing CdSe nanorods and a 1:1 mixture of lauric acid (LA) and hexadecylamine (HAD) (see the Supporting Information for experimental details). Heating this mixture at 80 °C under 3 bar H_2 for 24 h results in the growth of spherical cobalt nanoparticles of mean diameter of 4.5 nm and narrow size distribution, on the tips of the CdSe rods (NCs1, Figure 1). A dominance of one-sided growth is observed at this growth stage, although two-sided growth of Co spheres is also identified.

Under these conditions, simultaneous homogeneous nucleation of cobalt nanoparticles also occurs. Transmission electron microscopy (TEM) images show the presence of small free Co nanoparticles much smaller than the Co

[*] Prof. M. Respaud, Dr. K. Soulantica
Université de Toulouse; INSA, UPS, LPCNO
135 avenue de Rangueil, 31077 Toulouse (France)
and
CNRS; LPCNO
31077 Toulouse (France)
Fax: (+33) 5-6155-9697
E-mail: ksoulant@insa-toulouse.fr
Dr. J. Maynadié, Dr. B. Chaudret
Laboratoire de Chimie de Coordination; CNRS
205 route de Narbonne, 31077, Toulouse (France)
and
Université deToulouse; UPS, INPT, LCC
31077 Toulouse (France)
A. Salant, E. Shaviv, Prof. U. Banin
Institute of Chemistry and The Center of Nanoscience and Nanotechnology, The Hebrew University of Jerusalem
Jerusalem 91904 (Israel)
Dr. A. Falqui
Istituto Italiano di Tecnologia
Via Morego 30, 16163 Genova (Italy)

[**] The authors thank the European project SA-NANO (Contract No. STRP 013698) for financial support, A. Mari for SQUID measurements, Dr. P. Lecante for XRD, and TEMSCAN service for the microscopy.

Supporting information for this article is available on the WWW under http://dx.doi.org/10.1002/anie.200804798.

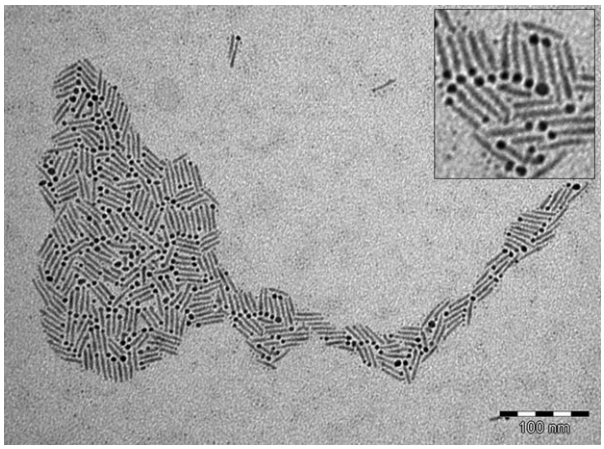

Figure 1. TEM images of Co-tipped CdSe nanorods NCs1 after 24 h reaction at 80 °C. Inset shows a magnified area of about 100×100 nm.

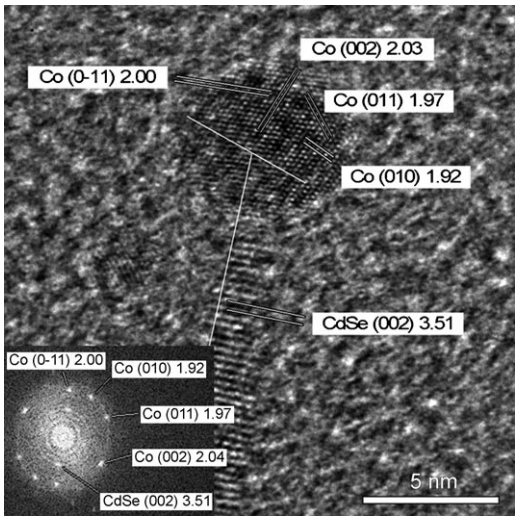

Figure 2. HREM image: Cobalt is strained in an initial phase of growth on the tip of cadmium selenide rod. The inset shows the 2D fast Fourier transform of the upper part of HREM and corresponding indexes (see the Supporting Information). The [002] directions in the CdSe and Co domains are indicated by the superposed long thin white lines. Plane distances are given in Å.

nanoparticles located on the CdSe rod tips; this side product could be separated from the CdSe–Co sample by centrifugation. However, control experiments provide strong evidence that the NCs1 structures are formed by heterogeneous growth of Co on CdSe and not by an oriented attachment of preformed Co nanoparticles (see the Supporting Information).

When the concentration of ligands was increased relative to Co, a decrease in the number of Co-tipped CdSe rods was observed. When both Co and ligand concentrations were reduced relative to the concentration of CdSe rods, Co particles grew with a very inhomogeneous size distribution. In this case, several Co particles grown on the lateral sides of the CdSe rods were observed. (see the Supporting Information). Furthermore, washing tetradecylphosphonic acid away from the CdSe surface prior to HDA/LA addition while keeping the other parameters stable causes Co to grow nonselectively on the CdSe as well as away from it. These observations suggest that the coordination of the ligands along the side of CdSe rods plays a role in directing the growth of the Co particles.[5b] Moreover, dominance of one-sided growth is seen for this reaction, even at short growth times (see the Supporting Information).[3b]

Selected area electron diffraction, X-ray diffraction measurements (see the Supporting Information), and high-resolution electron microscopy (HREM) analyses show clearly that CdSe nanorods grow with a wurtzite structure and along the [002] crystallographic direction, almost always with nonplanar tips. The Co structure is also hexagonal, but its lattice constants are quite different from CdSe. As a result, the Co particles are strained (Figure 2). A full analysis of the HREM results is given in the Supporting Information.

After purification of the Co-tipped CdSe rods from unreacted molecular cobalt species and small cobalt nanoparticles, the optical and magnetic properties of NCs1 were studied. The optical absorption and photoluminescence (PL) spectra of NCs1 and the CdSe nanorods are shown in Figure 3a (experimental details are given in the Supporting Information). Upon Co growth, the absorption onset exhibits a tail to the red, and the excitonic feature of the original CdSe

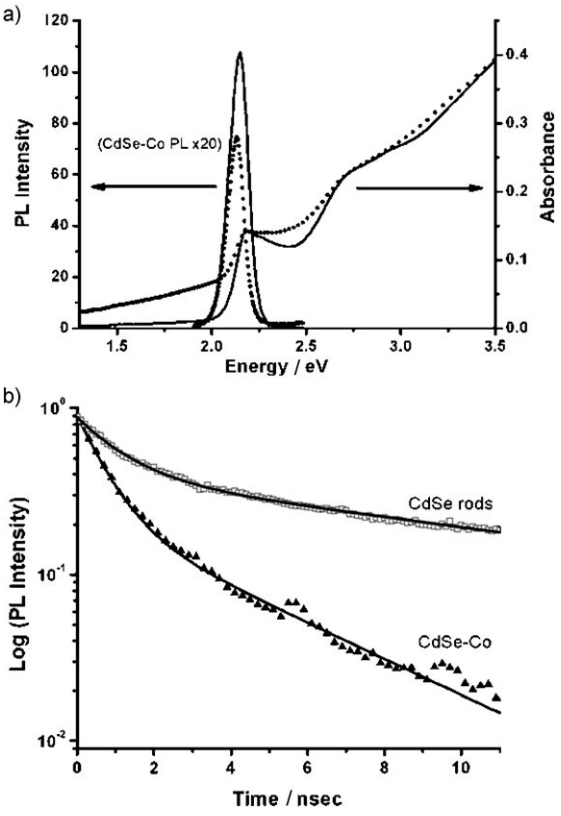

Figure 3. a) Absorption and photoluminescence spectra of "treated" CdSe nanorods (——) and NCs1 (•••••). Emission was measured with excitation at 400 nm. The emission from the CdSe–Co structures (NCs1) is multiplied by 20 for clarity. b) Time-resolved PL of "treated" nanorods (□, $\tau_1 = 1.1$ ns, $\tau_2 = 14$ ns) and NCs1 (▲, $\tau_1 = 0.7$ ns, $\tau_2 = 4$ ns), excited at 400 nm. Original data (□, ▲) and fit to a biexponential decay (——) are presented.

nanorods is broadened. In comparison, for CdSe–Au hybrid nanoparticles,[3a] the excitonic feature is washed out rapidly with Au growth. This difference might be attributed to the closer overlap of the Au plasmon feature and the CdSe exciton peak compared to the CdSe–Co system. The emission intensity of NCs1 dropped upon Co growth and was found to be 30 times lower than that of "treated" CdSe nanorods that were exposed to the same synthetic procedure without the presence of Co.

PL lifetimes were measured to determine the origin of the detected emission (Figure 3b). The measured data was fit to a biexponential decay. Both components of the PL lifetime for NCs1 were found to be shorter than those of "treated" CdSe nanorods ($\tau_1 = 1.1$ ns, $\tau_2 = 14$ ns for CdSe vs. $\tau_1 = 0.7$ ns, $\tau_2 =$ 4 ns for NCs1). This result implies that the detected emission originates from NCs1 and not from residues of bare CdSe that may have remained in the sample, as in the latter case the lifetime dynamics should not change. We assume that the PL quenching upon Co growth is due to the appearance of a new nonradiative pathway arising from the interaction between the semiconductor and the metal. It is noteworthy that upon Au growth on CdSe, even more complete quenching of the PL was observed.[3a] This quenching was assigned to electron transfer from the conduction band of CdSe to the Au tip.[10] The Fermi level of Co is located approximately 0.4 eV below the conduction band of CdSe, similar to the case of CdSe–Au.[10,11] Such an energy band alignment of the hybrid nanocrystals would allow electron transfer from the excited semiconductor to the metal tip, which should lead to lifetime shortening, as indeed observed. It is interesting to note that the determined lifetime of 4 ns for NCs1 is close to that reported for core/shell Co–CdSe nanocrystals. The authors of that report suggested that the PL quenching could be due to alteration of the spin structure of the lowest excitonic state owing to the proximity of the Co metal.[12]

The magnetic properties of NCs1 were studied by superconducting quantum interference device (SQUID) magnetometry. Interestingly, the cobalt maintains its magnetic properties. As can be seen in Figure 4a, the saturation magnetization (M_S) measured at 2 K is just below the bulk value (163 $A\,m^2\,kg_{Co}^{-1}$). The hysteresis curves at 2 K, either after a zero field cooling (ZFC) or a field cooling (FC) at 5 T from 300 K, above the Néel temperature of Co oxides, are exactly the same. The absence of exchange phenomena allows us to exclude the presence of a Co oxide layer. As a consequence of the nanometric size of the Co nanospheres, a superparamagnetic transition is induced by the temperature, with a blocking temperature of $T_b = 150$ K (see the Supporting Information). The experimental curve can be well fitted considering the Langevin function and the Gaussian size distribution estimated from the TEM micrographs.[13] Finally, we used the blocking temperature and the mean particle volume $\langle v \rangle$ to deduce the effective anisotropy $K_{eff} = 25\,k_B\,T_b/\langle v \rangle = (5.0 \pm 1) \times 10^5\ J\,m^{-3}$. This value, which is in the same range as for pure Co nanoparticles of comparable size, is one of the largest ever obtained in such nanoobjects combining a quantum dot and a magnetic nanoparticle, either as core/shell particles or as heterodimers.[3d,14]

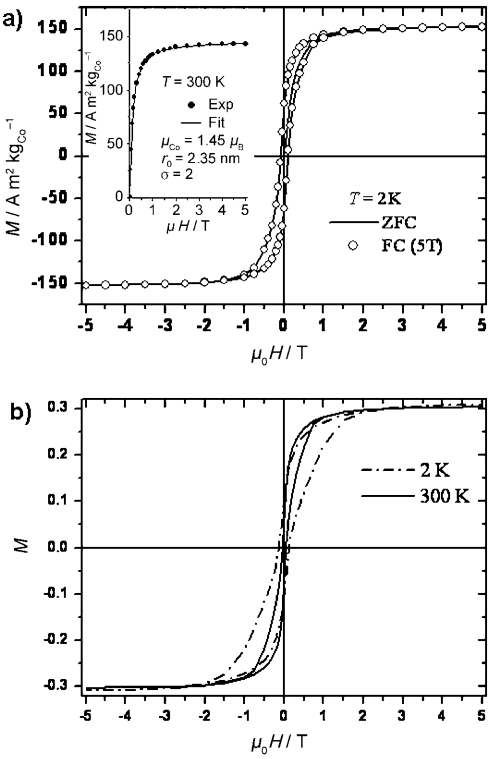

Figure 4. Magnetic properties: a) NCs1: ZFC and FC hysteresis curves at 2 K and magnetization curve at 300 K with its fitting; b) NCs2: ZFC hysteresis curves measured at 2 and 300 K.

The formation of hybrid nanoparticles opens new opportunities for the preparation of novel materials, as demonstrated below by the synthesis of cobalt nanorods attached to CdSe nanorods (NCs2). These heterostructures are obtained when the synthesis temperature is increased to 100 °C while all other parameters are kept the same as in the reaction to form NCs1 (Figure 5). CdSe rods with spherical Co tips with mean diameter of 8.5 nm are also present. It is noteworthy that prolonging the reaction at 80 °C also leads to anisotropic

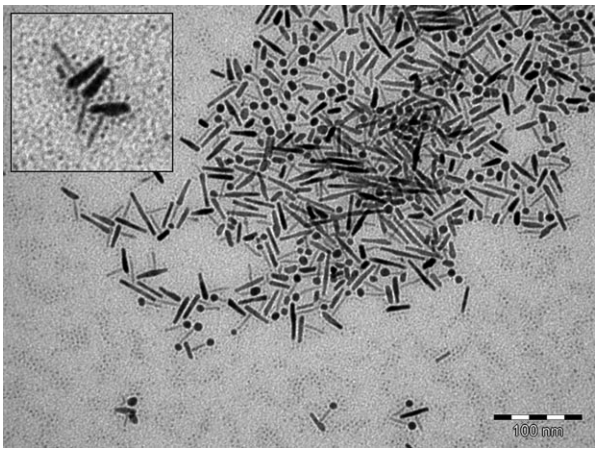

Figure 5. NCs2 after 24 h reaction at 100 °C; scale bar 100 nm. The inset shows another area of about 100 nm × 100 nm.

growth of the initially spherical Co nanoparticles. The reaction carried out at 100 °C for 5 h shows the presence of nanospheres, and therefore we infer that these are intermediates on the way to the growth of Co nanorods (see the Supporting Information).

The HREM analysis of NCs2 shows that the cobalt grows along its [002] direction and relaxes slowly upon growth. In the final NCs2 product, the Co adopts its bulk hexagonal close-packed (hcp) lattice constant (see the Supporting Information). As already observed by TEM, HREM analysis clearly indicates that the Co grows on the CdSe tip along four orientations only. These different orientations between Co and CdSe nanorods, shown in the HREM images of Figure SI.8 in the Supporting Information, are distinguished by four different angles β (112 ± 3, 135 ± 3, 6 ± 3, and $99 \pm 3°$), between the two [002] growth directions of CdSe and Co. These repetitive structural relationships are due to the great difference between cobalt and CdSe hcp lattice constants: a crystallographic tilting is necessary to allow the cobalt lattice to grow on the nonplanar tip of the CdSe rod, that is, to minimize the lattice mismatch between Co and CdSe. It is therefore not unlikely that the nanorod–nanosphere object of Figure 2 corresponds, to a "precursor" of a NC2 structure of type a in Figure SI.8 in the Supporting Information ($\beta = 112°$). It is expected that the four orientations detected for NCs2 are already present from the beginning of growth, that is, in NCs1. Indeed, an HREM analysis of several NCs1 structures revealed three out of the four orientations detected in NCs2. In Figure SI.9 in the Supporting Information, we show the cases of NCs1 that correspond to the "precursors" of NCs2 of the types c ($\beta = 6°$) and d ($\beta = 99°$) in Figure SI.8 in the Supporting Information.

For NCs2 after purification, the magnetization curves display a hysteretic behavior even at room temperature (Figure 4b). This finding is expected considering the size of the Co objects (either nanospheres or nanorods). To our knowledge, these are the first magnetic–semiconducting heterostructures that are ferromagnetic at room temperature.

In conclusion, we have prepared new CdSe–Co semiconducting–magnetic hybrid nanocrystals and have demonstrated for the first time the possibility to grow a magnetic metal anisotropically on the tip of a semiconductor nanorod. Regarding their optical properties, the NCs1 structures remain fluorescent, however, their emission quantum yield is considerable lower than the template CdSe nanorods. We show that the NCs1 structures display similar magnetic properties to pure Co nanoparticles of the same size, with large magnetization and effective magnetic anisotropy. By changing the particle size and geometry, we can tune the magnetic properties at room temperature either with superparamagnetic or ferromagnetic tips, which may widen the field of applications of such hybrid nanoparticles. A limitation of the possible angles between the magnetic and semiconducting nanorods could enable the orientation of such hybrid nanoobjects by application of an external magnetic field and their organization over large areas.

Received: October 1, 2008
Published online: January 28, 2009

Keywords: heterostructures · magnetic properties · nanorods · nanostructures · semiconductors

[1] a) J. Hu, L.-S. Li, W. Yang, L. Manna, L.-W. Wang, A. P. Alivisatos, *Science* **2001**, *292*, 2060–2063; b) S. Sun, C. B. Murray, D. Weller, L. Folks, A. Moser, *Science* **2000**, *287*, 1989–1992; c) J. Park, J. Joo, S. G. Kwon, Y. Jang, T. Hyeon, *Angew. Chem.* **2007**, *119*, 4714–4745; *Angew. Chem. Int. Ed.* **2007**, *46*, 4630–4660; d) A. R. Tao, S. Habas, P. Yang, *Small* **2008**, *4*, 310–325.

[2] a) P. D. Cozzoli, T. Pellegrino, L. Manna, *Chem. Soc. Rev.* **2006**, *35*, 1195–1208; b) H. Zeng, S. Sun, *Adv. Funct. Mater.* **2008**, *18*, 391–400.

[3] a) T. Mokari, E. Rothenberg, I. Popov, R. Costi, U. Banin, *Science* **2004**, *304*, 1787–1790; b) T. Mokari, C. G. Sztrum, A. Salant, E. Rabani, U. Banin, *Nat. Mater.* **2005**, *4*, 855–863; c) S. Kudera, L. Carbone, M. F. Casula, R. Cingolani, A. Falqui, E. Snoeck, W. J. Parak, L. Manna, *Nano Lett.* **2005**, *5*, 445–449; d) H. Gu, R. Zheng, X. Zhang, B. Xu, *J. Am. Chem. Soc.* **2004**, *126*, 5664–5665; e) J. Choi, Y. Jun, S. Yeon, H. C. Kim, J. S. Shin, J. Cheon, *J. Am. Chem. Soc.* **2006**, *128*, 15982–15983; f) C. Xu, J. Xie, D. Ho, C. Wang, N. Kohler, E. G. Walsh, J. R. Morgan, Y. E. Chin, S. Sun, *Angew. Chem.* **2008**, *120*, 179–182; *Angew. Chem. Int. Ed.* **2008**, *47*, 173–176.

[4] a) H. Yu, P. C. Gibbons, K. F. Kelton, W. E. Buhro, *J. Am. Chem. Soc.* **2001**, *123*, 9198–9199; b) .J. P. Wilcoxon, P. P. Provencio, *J. Am. Chem. Soc.* **2004**, *126*, 6402–6408.

[5] a) A. E. Saunders, I. Popov, U. Banin, *J. Phys. Chem.* **2006**, *110*, 25421–25429; b) F. Wetz, K. Soulantica, A. Falqui, M. Respaud, E. Snoeck, B. Chaudret, *Angew. Chem.* **2007**, *119*, 7209–7211; *Angew. Chem. Int. Ed.* **2007**, *46*, 7079–7081.

[6] A. Salant, E. Amitay-Sadovsky, U. Banin, *J. Am. Chem. Soc.* **2006**, *128*, 10006–10007.

[7] W. U. Huynh, J. J. Dittmer, A. P. Alivisatos, *Science* **2002**, *295*, 2425–2427.

[8] S. Habas, P. Yang, T. Mokari, *J. Am. Chem. Soc.* **2008**, *130*, 3294–3295.

[9] a) W. Shi, H. Zeng, Y. Sahoo, T. Y. Ohulchanskyy, Y. Ding, Z. L. Wang, M. Swihart, P. N. Prasad, *Nano Lett.* **2006**, *6*, 875–881; b) W. Shi, Y. Sahoo, H. Zeng, Y. Ding, M. T. Swihart, P. N. Prasad, *Adv. Mater.* **2006**, *18*, 1889–1894.

[10] R. Costi, A. E. Saunders, E. Elmalem, A. Salant, U. Banin, *Nano Lett.* **2008**, *8*, 637–641.

[11] a) D. S. Ginger, N. C. Greenham, *J. Appl. Phys.* 2000, 87, 1361–1368; b) M. V. Tiba, W. J. M. de Jonge, B. Koopmans, H. T. Jonkman, *J. Appl. Phys.* **2006**, *100*, 093707.

[12] H. Kim, M. Achermann, L. P. Balet, J. A. Hollingsworth, V. I. Klimov, *J. Am. Chem. Soc.* **2005**, *127*, 544–546.

[13] The Langevin equation is given by $m(H) = M_S(T)\mathrm{L}\left(\frac{M_S(T)\,v\,H}{k_B\,T}\right)$, $\mathrm{L}(x) = \coth(x) - \frac{1}{x}$ where v is the particle size, T the temperature, k_B the Boltzman constant, and H the applied magnetic field.

[14] J. Gao, B. Zhang, Y. Gao, Y. Pan, X. Zhang, B. Xu, *J. Am. Chem. Soc.* **2007**, *129*, 11928–11935.

